Journal of Electron Spectroscopy and Related Phenomena 198 (2015) 1–5

Contents lists available at ScienceDirect

Journal of Electron Spectroscopy and Related Phenomena

journal homepage: www.elsevier.com/locate/elspec

Tight-binding approach to understand photoelectron intensity from graphene for circularly polarized light

Hwihyeon Hwang, Choongyu Hwang*

Department of Physics, Pusan National University, Busan 609-735, Republic of Korea

ARTICLE INFO

Article history:
Received 4 June 2014
Received in revised form
22 September 2014
Accepted 31 October 2014
Available online 11 November 2014

Keywords:
Circular dichroism
Imperfect circular polarization
Photoemission spectroscopy
Graphene
Tight-binding formalism

ABSTRACT

We have investigated the effect of imperfect circular polarization on the angle-resolved photoemission spectroscopy signal, using graphene as a prototypical system that can be understood within tight-binding formalism. We found that perfect left- and right-circularly polarized lights give the same photoelectron intensity distribution around a constant energy contour of the graphene π band. On the other hand, upon breaking the purity of the polarization, photoelectron intensity starts to show circular dichroism, which is enhanced with further increasing the imperfection. Our results predict the existence of an additional factor for the circular dichroism observed in the photoemission signal from graphene and hence suggest the importance of experimental conditions to understand circular dichroism observed via photoemission spectroscopy.

1. Introduction

Circular dichroism has been one of the powerful methodologies to extract information on spin and/or orbital properties of charge carriers in solid state systems [1–3]. In addition, recent study on graphene has suggested that information on Berry phase can also be obtained via the circular dichroism [4], extending a previous approach of the direct measurement of Berry phase using linearly polarized lights for the same system [5]. These results provide an experimental evidence that the quantum mechanical phases can be probed by photoemission spectroscopy, previously not believed to be possible, and hence constitute the first band specific measurements of Berry phase.

These interesting observations have been possible due to the simple geometric structure of graphene, allowing us to obtain the explicit form of the initial electronic states within the tight-binding formalism [6]. Shirley et al. [7], calculated photoelectron intensity, which is the absolute square of the transition matrix element $M_k = \langle f_{\mathbf{k}}|H^{\mathrm{int}}(\mathbf{k})|\psi_{\mathbf{k}}\rangle$, where $|\psi_{\mathbf{k}}\rangle$ is a tight-binding eigenstate, $|f_{\mathbf{k}}\rangle$ is a plane-wave final state, and $H^{\mathrm{int}} = \mathbf{A}\cdot\mathbf{p}$. Here, $\mathbf{A}$ is a light polarization and $\mathbf{p} = -i\hbar\nabla$ is the momentum operator, where $\hbar$ is the Planck's constant.

This approach reproduces the photoelectron intensity for the linearly polarized light along the x-axis denoted in Fig. 1(a), i.e., X-polarization ($\mathbf{A} = A_x\hat{\mathbf{x}}$), whereas it is not successful in reproducing full polarization dependence of the photoelectron intensity, e.g., when the light polarization is rotated by 90°, i.e., Y-polarization ($\mathbf{A} = A_y\hat{\mathbf{y}}$) [5]. This issue originates from the application of $\mathbf{p} = -i\hbar\nabla$ to the tight-binding eigenstates. When the tight-binding Hamiltonian is intrinsically non-local, the derivative in real space for the tight-binding eigenstate does not work [8,9]. This suggests that the agreement even for X-polarization using $\mathbf{p}$ [7] could be fortuitous. In order to solve this issue, Hwang et al. [5] introduced an alternative approach replacing the derivative to the commutation relation, i.e., $\mathbf{p}/m_0 = -i\hbar\nabla/m_0$, where m_0 is free-electron mass, to $\mathbf{v} = [\mathbf{r}, H^0]/i\hbar$, where $\mathbf{r} = i\hbar(\nabla_{\mathbf{k}}, \partial_{k_z})$ in the $\mathbf{k}$-representation [9,10].

To avoid this issue, Liu et al., have assumed realistic final states, i.e., the Block sum of the Wannier states, while still using $\mathbf{p}$ [4]. With this setup, they have claimed that the observed circular dichroism originates from Berry phase of graphene, which is challenged by a study on the circular dichroism as a function of electron binding energy [11]. In fact, another experimental study shows that the circular dichroism varies upon changing photon energy, emphasizing the role of the final state effect in understanding photoemission signal from graphene [12]. These controversies give rise to a fundamental question on the origin of the circular dichroism.

Here we report calculated photoelectron intensity of graphene for circularly polarized light. The photoemission matrix element was constructed using the velocity operator [5,9] within the

* Corresponding author. Tel.: +82 515102961.
E-mail address: ckhwang@pusan.ac.kr (C. Hwang).

http://dx.doi.org/10.1016/j.elspec.2014.10.011
0368-2048/

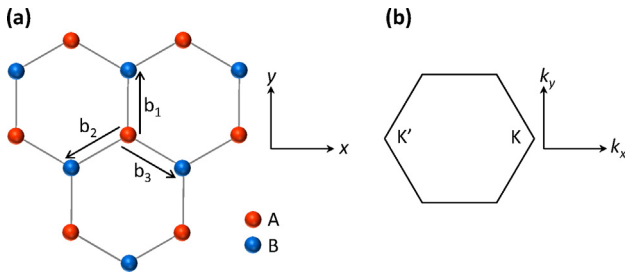

Fig. 1. (a) Schematic of graphene in real space. (b) The first Brillouin zone of graphene. Here, $\mathbf{b}_1 = b(0, 1)$, $\mathbf{b}_2 = b(-\sqrt{3}/2, -1/2)$ and $\mathbf{b}_3 = b(\sqrt{3}/2, -1/2)$ are the three vectors connecting the in-plane nearest neighbor atoms where $b = 1.42$ Å. The positions of the K and K′ points are $(4\pi/3a, 0)$ and $(-4\pi/3a, 0)$, respectively, where $a = \sqrt{3}b$.

tight-binding formalism. We found that the photoelectron intensity for left- and right-circularly polarized light (LCP and RCP, respectively) does not show any difference for perfect circular polarization. On the other hand, upon decreasing the purity of the polarization, the photoelectron intensity starts to exhibit circular dichroism. Our results indicate that an experimental condition in conjunction with the intrinsic effects such as the isospin of charge carriers and the final states [12] plays an important role in determining photoelectron intensity.

2. Tight-binding formalism

Fig. 1(a) shows the geometric structure of graphene with two carbon sublattices, A and B. In order to describe the electron energy eigenvalues and wavefunctions, we have used tight-binding formalism for the p_z orbital of each sublattice using the in-plane nearest-neighbor (A-B) hopping integral, t_0 (we confine our interest to this single parameter for simplicity), which corresponds to $-\gamma_0'$ in the well-known Slonczewski–Weiss–McClure model [14,15]. Because our basis set for the tight-binding model has more than one non-equivalent orbitals, there exist two different hopping parameters differing only in the sign that give exactly the same electron band structure. In this sense, the absolute magnitude of inter-orbital hopping integrals within the empirical tight-binding Hamiltonian H_{TB} between non-equivalent states (i.e., $\langle\phi_1|H_{\mathrm{TB}}|\phi_2\rangle$, where the localized orbitals $|\phi_1\rangle$ and $|\phi_2\rangle$ are not equivalent) in any material have only been speculated theoretically, whereas it has recently been proved that the sign of the hopping integrals for both single- and double-layer graphene can be experimentally determined uniquely using the angle-resolved photoemission spectroscopy (ARPES) technique [5]. We have used $|t_0| = 3.16$ eV and $t_0 < 0$, the values in Table II of Grüneis et al., [13] and in Fig. 8 of Hwang et al. [5], respectively.

The tight-binding Hamiltonian of graphene for two-dimensional wavevector $\mathbf{k}$ is as follows [5,6]:

$$H^0(\mathbf{k}) = \begin{pmatrix} 0 & t_0 g(\mathbf{k}) \\ t_0\, g^*(\mathbf{k}) & 0 \end{pmatrix}, \tag{1}$$

using a basis set composed of Bloch sums of localized orbitals on each sublattice:

$$g(\mathbf{k}) = \sum_{i=1}^{3} \exp(i\mathbf{k}\cdot\mathbf{b}_i) \tag{2}$$

with $\mathbf{b}_i$'s defined as in Fig. 1(a), and

$$\begin{pmatrix} 1 \\ 0 \end{pmatrix}_{\mathbf{k}} = \frac{1}{\sqrt{N}} \sum_{\mathbf{R}_{\mathrm{A}}} e^{i\mathbf{k}\cdot\mathbf{R}_{\mathrm{A}}} \phi(\mathbf{r} - \mathbf{R}_{\mathrm{A}}), \tag{3}$$

$$\begin{pmatrix} 0 \\ 1 \end{pmatrix}_{\mathbf{k}} = \frac{1}{\sqrt{N}} \sum_{\mathbf{R}_{\mathrm{B}}} e^{i\mathbf{k}\cdot\mathbf{R}_{\mathrm{B}}} \phi(\mathbf{r} - \mathbf{R}_{\mathrm{B}}). \tag{4}$$

In the presence of the vector potential $\mathbf{A}$, the Hamiltonian is obtained by Peierls substitution, i.e., $\mathbf{k} \to \mathbf{k} - (e/\hbar c)\mathbf{A}$. Then, the interaction Hamiltonian H^{int} is obtained by the first-order term of $\mathbf{A}$ from $H^0(\mathbf{k} - (e/\hbar c)\mathbf{A}) - H^0(\mathbf{k})$, and represented as $-(e/c)\hat{\mathbf{A}}\cdot\hat{\mathbf{v}}$ using the velocity operator $\hat{\mathbf{v}} = [\hat{\mathbf{r}}, \hat{H}^0]/i\hbar$, where $\hat{\mathbf{r}} = i\hbar\nabla_{\mathbf{k}}$ in the $\mathbf{k}$-representation, $\hbar$ is the Planck's constant, e is the charge of an electron, and c is the speed of light. Then the interaction Hamiltonian becomes [5]:

$$H^{\mathrm{int}}(\mathbf{k}) = -\frac{e}{\hbar c}\mathbf{A}\cdot \begin{pmatrix} 0 & t_0\,\nabla_{\mathbf{k}} g(\mathbf{k}) \\ t_0\,\nabla_{\mathbf{k}} g^*(\mathbf{k}) & 0 \end{pmatrix}. \tag{5}$$

Note here that because $g(\mathbf{k})$ depends only on the k_x and k_y components of the wavevector $\mathbf{k}$, there is no contribution arising from the z component of the vector potential A_z within this tight-binding model. In real measurements, the light with a nonzero polarization component along the z direction will give rise to an additive isotropic term to the photoelectron intensity that is independent of the in-plane polarization of the light.

3. The analysis of the photoelectron intensity

The photoelectron intensity is described by the absolute square of the transition matrix element $M_{s\mathbf{k}} = \langle f_{\mathbf{k}}|H^{\mathrm{int}}(\mathbf{k})|\psi_{s\mathbf{k}}\rangle$, where $|\psi_{s\mathbf{k}}\rangle$ is graphene eigenstate with the band index $s = \pm 1$ for conduction (+) and valence (−) bands, and $|f_{\mathbf{k}}\rangle$ is the plane-wave final state projected onto the p_z orbitals of graphene. For graphene, we may use

$$|f_{\mathbf{k}}\rangle = \frac{1}{\sqrt{2}} \begin{pmatrix} 1 \\ 1 \end{pmatrix}_{\mathbf{k}}. \tag{6}$$

Here, we neglect the k_z dependence of the final state, as done in the previous works [5,7,16]. For a few tens eV photons, typical for ARPES measurements for graphene [4,5,11,12,16,19], k_z of the plane-wave final state is much larger than k_x and k_y, leading to only a small variation in k_z with any change in k_x and k_y. In addition, the study on k_z, i.e., photon energy dependence, is beyond the capability of the tight-binding formalism, but can be achieved through the first principles calculations [12].

When we consider the case where $\mathbf{k}$ is very close to the Dirac point $\mathbf{K}$ as denoted in Fig. 1(b), and define $\mathbf{q} = \mathbf{k} - \mathbf{K}$ ($|\mathbf{q}| \ll |\mathbf{K}|$), Eq. (2) becomes

$$g(\mathbf{q} + \mathbf{K}) \approx -\frac{\sqrt{3}}{2} b(q_x - iq_y), \tag{7}$$

and the Hamiltonians become

$$H^0(\mathbf{q} + \mathbf{K}) \approx -\frac{\sqrt{3}}{2}\, b\, t_0 (q_x \sigma_x + q_y \sigma_y), \tag{8}$$

and

$$H^{\mathrm{int}}(\mathbf{q} + \mathbf{K}) \approx \frac{\sqrt{3}e}{2\hbar c}\, b\, t_0\, (\mathbf{A}\cdot\boldsymbol{\sigma}), \tag{9}$$

where σ is the Pauli matrix. Then the electron energy eigenvalues and wavefunctions of the H^0 are given by $E_{s\mathbf{k}} = \sqrt{3}/2\, b\, |t_0|\, s\, |\mathbf{q}|$ and

$$|\psi_{s\mathbf{k}}\rangle = \frac{1}{\sqrt{2}} \begin{pmatrix} e^{-i\theta_{\mathbf{q}}/2} \\ s\, e^{i\theta_{\mathbf{q}}/2} \end{pmatrix}, \tag{10}$$

respectively, when $\theta_{\mathbf{q}}$ is the angle between $\mathbf{q}$ and the $+k_x$ direction. With this setup, the photoemission matrix elements for X- and Y-polarizations are given by

$$M_{+1\mathbf{k}}^{\mathrm{X-pol.}} \sim \exp\left(\frac{-i\theta_{\mathbf{q}}}{2}\right) + s\exp\left(\frac{i\theta_{\mathbf{q}}}{2}\right), \tag{11}$$

and

$$M_{+1\mathbf{k}}^{\mathrm{Y-pol.}} \sim \exp\left(\frac{-i\theta_{\mathbf{q}}}{2}\right) - s\exp\left(\frac{i\theta_{\mathbf{q}}}{2}\right), \tag{12}$$

respectively, of which absolute square, i.e., $I_{s\,k} = |M_{s\,k}|^2$, represents photoelectron intensity that reproduces the previous experimental results for linearly polarized lights [4,5]. Resultantly, the variation of photoelectron intensity depending on the polarity of light reveals the pseudospin nature of charge carriers in single- and double-layer graphene, i.e., Berry phase of π and 2π, respectively, and the signs of hopping integral in the tight-binding Hamiltonian for double-layer graphene or graphite [5].

In the same analogy, for the circularly polarized light, i.e., $\mathbf{A} = A_x\,\hat{x} \pm i\,A_y\,\hat{y}$, the photoemission matrix element is given by

$$M_{s\mathbf{k}} = \frac{A_x}{2}\left(s\,\exp\left(\frac{i\theta_{\mathbf{q}}}{2}\right) + \exp\left(\frac{-i\theta_{\mathbf{q}}}{2}\right)\right) \pm \frac{A_y}{2}\left(s\,\exp\left(\frac{i\theta_{\mathbf{q}}}{2}\right) - \exp\left(\frac{-i\theta_{\mathbf{q}}}{2}\right)\right) \tag{13}$$

where + and − correspond to LCP and RCP, respectively. For the states above the Dirac energy, i.e., $s = +1$

$$M_{+1\mathbf{k}}^{\mathrm{LCP}} = A_x \cos\left(\frac{\theta_{\mathbf{q}}}{2}\right) + i\,A_y \sin\left(\frac{\theta_{\mathbf{q}}}{2}\right), \tag{14}$$

and

$$M_{+1\mathbf{k}}^{\mathrm{RCP}} = A_x \cos\left(\frac{\theta_{\mathbf{q}}}{2}\right) - i\,A_y \sin\left(\frac{\theta_{\mathbf{q}}}{2}\right), \tag{15}$$

and for the states below the Dirac energy, i.e., $s = -1$

$$M_{-1\mathbf{k}}^{\mathrm{LCP}} = -i\,A_x \sin\left(\frac{\theta_{\mathbf{q}}}{2}\right) + A_y \cos\left(\frac{\theta_{\mathbf{q}}}{2}\right), \tag{16}$$

and

$$M_{-1\mathbf{k}}^{\mathrm{RCP}} = -i\,A_x \sin\left(\frac{\theta_{\mathbf{q}}}{2}\right) - A_y \cos\left(\frac{\theta_{\mathbf{q}}}{2}\right). \tag{17}$$

It follows that

$$I_{+1\mathbf{k}} = A_x^2 \cos^2\left(\frac{\theta_{\mathbf{q}}}{2}\right) + A_y^2 \sin^2\left(\frac{\theta_{\mathbf{q}}}{2}\right), \tag{18}$$

and

$$I_{-1\mathbf{k}} = A_x^2 \sin^2\left(\frac{\theta_{\mathbf{q}}}{2}\right) + A_y^2 \cos^2\left(\frac{\theta_{\mathbf{q}}}{2}\right), \tag{19}$$

regardless of the chirality of the light. This simple algebra indicates that, within the tight-binding formalism for $|\mathbf{q}| \ll |\mathbf{K}|$, the photoelectron intensity of graphene does not show circular dichroism. Moreover, for perfect circular polarization, for which $|A_x| = |A_y|$, $I_{s\mathbf{k}}$ is isotropic around the constant energy contour. However, in real measurements, the photoelectron intensity for X- and Y-polarization geometries are different due to nonzero polarization component along the z direction, e.g., A_x exhibits a finite $\hat{z}$ component when projected to the sample surface, whereas A_y has negligible out-of-plane component [5], when the photoelectron intensity is closely related to the scattering probability of the real p_z orbitals for the out-of-plane component of light polarization, which is beyond the capability of the tight-binding approach. For example, at a photon energy of 50 eV, the ratio of $I_{\mathbf{k}}^{\mathrm{X-pol.}}/I_{\mathbf{k}}^{\mathrm{Y-pol.}}$ is ~21.4 [5] that we have used throughout our study. This ratio is not controllable, but determined for each experimental setup for each photon energy. This is also applied to the circular polarization, for which $\mathbf{A} = A_x\,\hat{x} \pm i\,A_y\,\hat{y}$ is projected onto the sample surface.

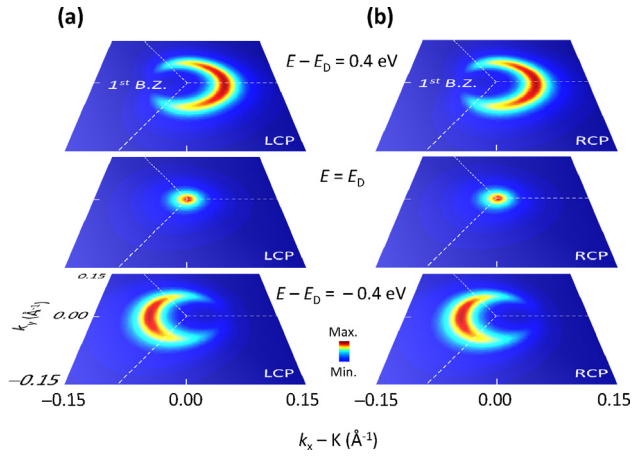

Fig. 2. Calculated photoelectron intensity of graphene for (a) left- and (b) right-circularly polarized lights. An arbitrary energy broadening of 0.10 eV has been used to qualitatively compare with experimental results [4,12].

These theoretical results are summarized in Fig. 2 at several different energies with respect to the Dirac energy, E_{D}. For LCP (Fig. 2(a)), the constant energy contour shows a crescent-like shape with minimum intensity in the first Brillouin zone (1st B.Z.) at $E - E_{\mathrm{D}} = 0.4$ eV and a point-like constant energy map at E_{D}. The intensity distribution is reversed at $E - E_{\mathrm{D}} = -0.4$ eV, with respect to E_{D}, with maximum intensity in the 1st B.Z. While the overall shape shows the characteristic conical dispersion of graphene, the intensity distribution is similar to the case of X-polarization [4,5]. It is important to note that, for linear polarizations, the crescent-like shape is understood by the interference between photoelectrons emitted from two carbon sublattices [7]. On the other hand, for circular polarizations, it originates from the relatively weak photoelectron intensity for Y-polarization as discussed above. As a result, the difference in photoelectron intensity between LCP and RCP is not determined by the properties of initial states, but given by the experimental geometry, and hence we expect the same intensity distribution for RCP as shown in Fig. 2(b).

Note also that our results (Eqs. (14), (15) and (18)) for the conduction band are different from those in the previous study (Eq. (3) of the Ref. [4]):

$$I = \left|A_x\xi_x(e^{i\theta/2} + e^{-i\theta/2}) \pm i\,A_y\xi_y(e^{i\theta/2} - e^{-i\theta/2})\right|^2, \tag{20}$$

where + and − signs correspond to LCP and RCP, respectively. In this study [4], they have claimed that the dipole transition matrix elements ξ_x and ξ_y for the x and y components of the vector potential have a relation of $\xi_x \approx \xi_y$ at 30 eV [17]. This setup results in

following photoelectron intensity (Eq. (4) of Ref. [4]) for the perfect circular polarization, i.e., $|A_x| = |A_y| \equiv |A|$,

$$I = 4|\xi_x|^2 A^2 \left| \cos\left(\frac{\theta}{2}\right) \pm \sin\left(\frac{\theta}{2}\right) \right|^2. \quad (21)$$

The difference between the two theoretical approaches (Eq. (18) vs. Eq. (21)) originates from the evolution of the tight-binding Hamiltonian. For example, for $|\mathbf{q}| \ll |\mathbf{K}|$, the Hamiltonian is expressed via Pauli matrices, i.e., $H = v_F \vec{\sigma} \cdot \vec{q}$ (Eq. (8)), where v_F is the Fermi velocity, with which we can obtain the tight-binding eigenstates (used in both works done by us (Eq. (10)) and Liu et al. [4]). Hence, the Peierls substitution naturally leads to $H^{int} = \vec{\sigma} \cdot \vec{A}$ [6], both of which components exhibit a strong influence on the photoemission matrix element when applied to the spinor eigenstate of graphene [5] as we have done in our study. On the other hand, Liu et al. [4], have applied the local Hamiltonian, $H = \mathbf{p}^2/2m + V(\mathbf{r})$, to the tight-binding eigenstates (Eq. (10)) obtained by the nonlocal tight-binding Hamiltonian (Eq. (1)) [9]. Consequently, the y component of the matrix element differs by the imaginary number "i" arising from σ_y (compare Eqs. (14), (15) and (21)) resulting in the completely different photoelectron intensity distributions [this issue is eliminated when the realistic eigenstates, e.g., maximally localized Wannier functions obtained by *ab initio* calculations [18], are used in conjunction with the local Hamiltonian].

In real measurements, in contrast to our prediction, the photoelectron intensity from graphene exhibits circular dichroism [4,11,12]. The intensity maximum around a constant energy contour rotates by 180° upon changing the chirality of light with an energy of 30 eV [4]. Such a dichroic effect varies at different photon energies [12], which has been attributed to the symmetry of the final states (d-like partial waves above a photon energy of 52 eV and s or p-like partial waves below 52 eV [19]). The photon energy dependence suggests that, when the final state effect is minimized around 52 eV, the still observed circular dichroism originates from the psuedospin nature of charge carriers in graphene [12]. Another study shows that, at a similar photon energy of 50 eV, the circular dichroism changes as a function of electron binding energy, which suggests a possibility of many-body interactions as an origin of the observed dichroism [11]. The distinct dichroic effect for different experiments may suggest the existence of an extrinsic factor contributing to the circular dichroism that changes at different experimental geometries and photon energies, such as imperfect circular polarization. In fact, the polarization purity for LCP and RCP in the experimental work for the Berry phase scenario is ~80% [4].

In Fig. 3, we show the effect of the imperfect polarization on the rotation of intensity maximum upon changing the chirality of light. We assume that the angle between the photon incident and the electron detector angles is 55° (e.g., the experimental setup for the previous experiment [5]). Then the angle between the photon incident and the sample normal angles is determined by photon energies. For example, at 50 eV, where the **K** points is tilted by ~29° with respect to the sample normal, the angle between the photon incident and the sample normal angles is ~26° (14 and 31° for 30 and 70 eV photons, respectively). In addition, for imperfect circular polarization, the major axis of the elliptical polarization is tilted by ±45° for LCP and RCP, respectively, with respect to $+\hat{x}$ direction. As a result, the elliptical polarization $A_x \hat{x} \pm i A_y \hat{y}$ projected to the sample surface becomes $A_x \cos 26° \cos 45° \pm i A_y \cos 26° \sin 45°$ and $-A_x \sin 45° \pm i A_y \cos 45°$ along x- and y-axis, respectively, where $(1-(a-b)/(a+b)) \times 100\,\%$ defines the purity of the polarization. When the purity of the polarization is 100% (Fig. 3(a)), the intensity maximum around the constant energy contour at $E - E_D = 0.4$ eV stays the same upon changing the chirality of light as denoted by the white arrows. When the purity of the polarization decreases, the intensity maximum becomes separated as denoted by the white arrows in Fig. 3(b) giving rise to the circular dichroism. The circular dichroism becomes stronger with further decreasing purity of the polarization as shown in Fig. 3(c).

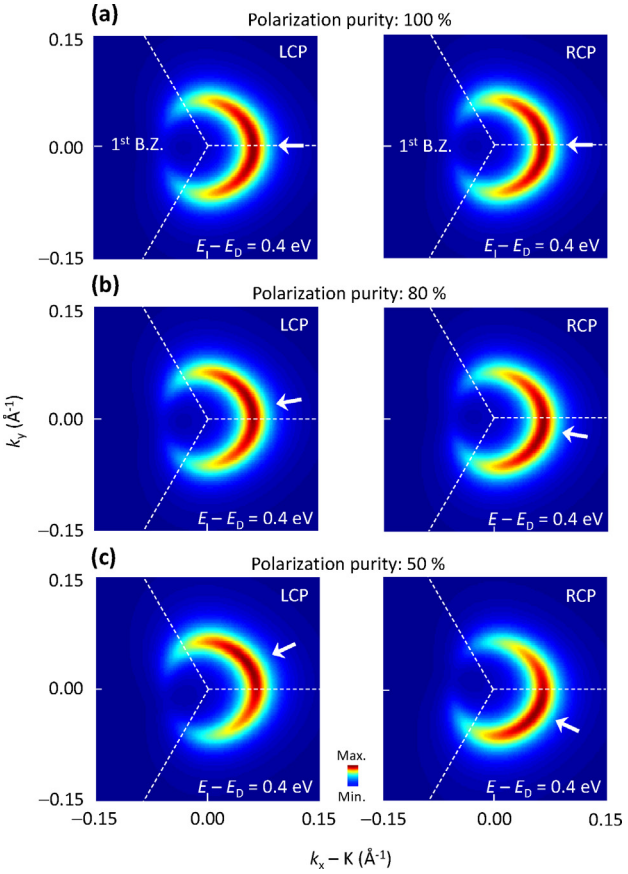

Fig. 3. Calculated photoelectron intensity of graphene for LCP (left panels) and RCP (right panels) at $E - E_D = 0.4$ eV for 100%, 80%, and 50% circular polarization. An arbitrary energy broadening of 0.10 eV has been used. The photon energy is assumed to be 50 eV and the angle of incident photons and surface normal is 26°, adapting the experimental geometry in Ref. [5].

To further discuss the discrepancy of our results compared to experimental results, we directly compare the rotational angles in both our and previous studies. When the final state effect is minimal at 52 eV [19], i.e., intrinsic properties of graphene dominate photoelectron intensities, the rotation of intensity maxima is only ~40° [12], different from the rotation by 180° corresponding to the Berry phase scenario [4]. While the tight-binding approach that we have used excellently reproduces the experimental data for linearly polarized light with an energy of 50 eV [5], the observed (~40°) and predicted (~60° via the first principles calculations) dichroism [12] is comparable to our result of 40–60° for the polarization purity of 80–50% (Fig. 3).

Now let us restrict our discussion to the case where the photon energy only changes photon polarization with respect to the sample surface. With this set up, we show the simulations for left-circularly polarized light with a polarization vector corresponding several photon energies (30, 50, and 70 eV in Fig. 4(a–c), respectively). Here, the angle between incident photons and the analyzer is assumed to be 55°. This simulation does not show a notable rotation of photoelectron intensity around a constant energy contour upon changing photon energy, suggesting that the final state effect [12] plays a dominant role in reproducing the photon energy dependence, while the experimental condition in conjunction with intrinsic effects, such as the pseudospin nature of charge carriers [12] and the many-body effects [11], also plays a finite role in

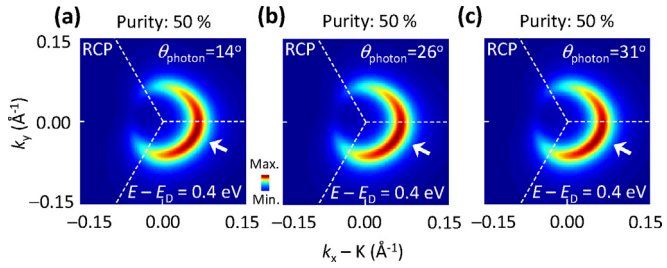

Fig. 4. Calculated photoelectron intensity of graphene for RCP at $E - E_D = 0.4$ eV. An arbitrary energy broadening of 0.10 eV has been used. The photon energy is assumed to be (a) 30, (b) 50, and (c) 70 eV, where the angle of incident photons and surface normal is 14°, 26°, and 31°, adapting the experimental geometry in Ref. [5].

rotating photoelectron intensity upon changing the chirality of light at constant photon energy. Overall, the theoretical approach within tight-binding formalism predicts an additional factor for the circular dichroism and hence suggests the importance of experimental conditions to understand circular dichroism observed via photoemission spectroscopy.

4. Conclusion

We have investigated the role of imperfect circular polarization in the circular dichroism of photoelectron intensity observed in graphene. Within the tight-binding formalism, we found that the calculated photoemission matrix element does not predict any difference between left- and right-circular polarization. However, we found that circular dichroism is developed and enhanced with decreasing purity of the polarization. Our results implies that the experimental conditions should be taken into account to understand circular dichroism, which invites further experimental and theoretical investigation to understand the origin of the observed circular dichroism in graphene.

Acknowledgements

We are greatly indebted to Cheol-Hwan Park and Sung-Kwan Mo for great help that has made this study possible. This work was supported by a 2-Year Research Grant of Pusan National University.

References

[1] W. Kuch, C.M. Schneiger, Rep. Prog. Phys. 64 (2001) 147.
[2] M. Polcik, et al., Phys. Rev. Lett. 92 (2004) 236103.
[3] M. Mulazzi, et al., Phys. Rev. B 74 (2006) 035119.
[4] Y. Liu, et al., Phys. Rev. Lett. 107 (2011) 166803.
[5] C. Hwang, et al., Phys. Rev. B 84 (2011) 125422.
[6] A.H. Castro Neto, et al., Rev. Mod. Phys. 81 (2009) 109.
[7] E.L. Shirley, L.J. Terminello, A. Santoni, F.J. Himpsel, Phys. Rev. B 51 (1995) 13614.
[8] A.F. Starace, Phys. Rev. A 3 (1971) 1242.
[9] S. Ismail-Beigi, E.K. Chang, S.G. Louie, Phys. Rev. Lett. 87 (2001) 087402.
[10] P.Y. Yu, M. Cardona, Fundamentals of Semiconductors: Physics and Materials Properties, Springer-Verlag, Berlin, Heidelberg, 1999.
[11] C. Hwang, J. Phys.: Condens. Matter 26 (2014) 335501.
[12] I. Gierz, et al., Nano Lett. 12 (2012) 3900.
[13] A. Grüneis, et al., Phys. Rev. B 78 (2008) 205425.
[14] J.C. Slonczewski, P.R. Weiss, Phys. Rev. 109 (1958) 272.
[15] J.W. McClure, Phys. Rev. 108 (1957) 612.
[16] M. Mucha-Kruczyński, et al., Phys. Rev. B 77 (2008) 195403.
[17] Liu et al., fitted experimental photoelectron intensity with two fitting parameters, β and λ, which are assumed to have a relation of $\lambda\, e^{i\beta} = \xi_y/\xi_x$, where ξ_y (ξ_x) is the matrix element for X- (Y-) polarization after taking out the phase factor ($e^{\pm i\theta/2}$) from the initial states [4]. Then, they have derived an explicit form of photoelectorn intensity to introduce Berry phase for the case of $\xi_y=\xi_x$, arguing that this is the case for a photon energy of 30 eV. However, at 30 eV, two fitting parameters give $\lambda \sim 0.7$ and $\beta \sim 0.1\pi$, denoting that $\xi_y/\xi_x \sim 0.67+0.22i$. This means that at least one of ξ_y and ξ_x is a complex quantity within their assumption, and that they are never the same. This raises a very important issue, because when one of them becomes a complex quantity, the calculated photoelectron intensity becomes completely different from the one derived by Liu et al. [4].
[18] N. Marzari, D. Vanderbilt, Phys. Rev. B 56 (1997) 12847.
[19] I. Gierz, et al., Phys. Rev. B 83 (2011) 121408(R).